Available online at BCREC Website: http://bcrec.undip.ac.id

Bulletin of Chemical Reaction Engineering & Catalysis, 10 (1), 2015, 23-29

Research Article

Selective Hydrogenation of Dibenzo-18-crown-6 ether over Highly Active Monodisperse Ru/γ-Al_2O_3 Nanocatalyst

Y.R. Suryawanshi[a,b], M. Chakraborty[a,*], S. Jauhari[b], S. Mukhopadhyay[c], K.T. Shenoy[c], D. Sen[d]

[a]*Chemical Engineering Department, S.V. National Institute of Technology, Surat-395 007, Gujarat, India*

[b]*Applied Chemistry Department, S.V. National Institute of Technology, Surat-395 007, Gujarat, India*

[c]*Chemical Engineering Division &* [d] *Solid State Physics Division, Bhabha Atomic Research Centre (BARC), Mumbai- 400085, Maharashtra, India*

[d] *Solid State Physics Division, Bhabha Atomic Research Centre (BARC), Mumbai- 400085, Maharashtra, India*

Received: 18th July 2014; Revised: 10th September 2014; Accepted: 10th September 2014

Abstract

Ru/γ-Al_2O_3 nanocatalyst with different metal loading was synthesized by microwave irradiated solvothermal technique. Synthesized nanocatalyst (4-14 nm of metal particle size) was then successfully implemented for the hydrogenation of dibenzocrown-18-crown-6 ether (DB18C6) at 9 MPa, 393 K temperature and 3.5 h. It was observed that the metallic small nanoclusters produced at 4 wt% metal concentration exhibited higher catalytic activity and resulted 96.7% conversion with 100% selectivity towards cis-syn-cis-dicyclohexano-18-crown-6 ether (CSC DCH18C6).

Keywords: ruthenium nanocatalyst; dibenzocrown-18-crown-6 ether; selective hydrogenation

How to Cite: Suryawanshi, Y.R., Chakraborty, M., Jauhari, S., Mukhopadhyay, S., Shenoy, K.T., Sen, D. (2015). Selective Hydrogenation of Dibenzo-18-crown-6 ether over Highly Active Monodisperse Ru/γ-Al_2O_3 Nanocatalyst. *Bulletin of Chemical Reaction Engineering & Catalysis*, 10 (1): 23-29. (doi:10.9767/bcrec.10.1.7141.23-29)

Permalink/DOI: http://dx.doi.org/10.9767/bcrec.10.1.7141.23-29

1. Introduction

Strontium-90 (^{90}Sr) is produced from nuclear reactor due to nuclear fission. It undergoes β^- decay into yttrium-90 and has half-life of 28.8 years. It is present in significant amount in spent nuclear fuel and in radioactive waste from nuclear reactors [1]. It is a heat generating nuclide and its removal from liquid waste stream is important for improved waste management strategies. Recovered Strontium 90 has applications in nuclear medicine and as compact power and heat source [2].

Crown ethers, a class of macrocyclic ligands, are found to be effective solvent as they possessed high affinity and selectivity for alkali and alkaline earth metal ions [3]. The selectivity in complexation of crown ether with a particular cation depends on the size of the ring and its stereochemistry. Reduction of Diben-

* Corresponding author:
E-mail address: mch@ched.svnit.ac.in (M. Chakraborty)
Tel.: +91 261 2201641; fax: +91 261 2227334

zocrown-18-crown-6 ether (DB18C6) produces five stereoisomers [cis-syn-cis (CSC), cis-anti-cis (CAC), trans-syn-trans (TST), trans-anti-trans (TAT), cis-trans (CT)] of dicyclohexano-18-crown-6 ether (DCH18C6) [4]. Literature shows that CSC DCH18C6 can extract radioactive ions more effectively from solutions of nuclear fuel reprocessing than other isomers [5,6]. As separation of different diasteoisomers is a complex and expensive process, so selective hydrogenation of DB18C6 to produce CSC DCH18C6 is worth considering. For stereoselective hydrogenation, various supported metal catalyst or colloidal metal particles were used. Pederson [7] carried out reduction of DB18C6 using Ru/Al_2O_3 catalyst under 70 atm of H_2 pressure but obtained a mixture of isomers. Laskorin *et al*. [8] obtained five isomers using Raney Ni catalyst. Gurskii *et al*. [9] used Ru, Rh, Pd and Pt catalysts supported on carbon and but failed to achieve selectivity towards CSC DCH18C6. Landre *et al*. used colloidal Rh catalyst and obtained 100% conversion, 86% chemoselectivity and syn:anti ratio 34:66 in presence of Aliquat-336 as phase transfer catalyst [10]. Recently, Gao *et al*. [11] carried out hydrogenation of DB18C6 using ruthenium nanocatalyst at 408 K and 10.0 MPa and obtained 99.4% conversion with 6:1 ratio of the syn/anti DCH18C6 as product.

From the above literature it has been found that ruthenium nanocatalyst shows high activity and stereoselectivity simultaneously due to its zero valence state and nano-scale size. Ru nanoparticles were synthesized by different methods such as microemulsion, solvothermal, sol-gel, co-precipitation, sonochemical reduction, microwave irradiation etc. Amongst this microwave irradiated solvothermal technique was found to be most effective as it is cleaner, greener, time saving and simple method of synthesis for metal nanoparticles. Zawadzki and Okal [12] and J. Okal [13] synthesized ruthenium nanoparticles by reduction of ruthenium chloride in ethylene glycol using a microwave assisted solvothermal method, dispersed on γ-Al_2O_3 and characterized by different technique. Recently, Antonetti *et al*. [14] reported synthesis of cabon nanotubes supported ruthenium nanoparticles using ethanol/water as solvent as well reducing agent under microwave irradiation. Rini *et al*. [15] synthesized Ru/γ-Al_2O_3 nanocatalyst by microwave irradiation technique in the presence and absence of stabilizer and characterized by different technique. Following the same line of action, in our previous study [16], we reported the microwave assisted synthesis of ruthenium nanoparticle using ethylene glycol as solvent and also as reducing agent. Effect of reaction temperature, time, PVP/$RuCl_3$ molar ratio and irradiation power on particle size and size distribution were also studied.

In this research work, we have synthesized Ru/γ-Al_2O_3 catalyst, dispersing ruthenium metal nanoparticles on γ-alumina support, characterized and also reported herein a straightforward and efficient catalyst system for challenging hydrogenation of DB18C6 to CSC DCH18C6 without adding any quaternary ammonium salt as phase transfer catalyst.

2. Experimental

2.1 Materials

Ruthenium trichloride ($RuCl_3.nH_2O$, Ru Content ≥ 37%), ethylene glycol (solvent) from Merck chemicals, India, Poly(N-vinyl-2-Pyrrolidone) (PVP as stabilizer, average molecular weight 40,000) from Heny fine chemicals, India, DB18C6 from sigma Aldrich India, γ-alumina powder, Al_2O_3 of 98% purity and 100 mesh size from National chemicals, India, commercial Ru/γ-Al_2O_3 (5 wt%) catalyst, acetone, n-BuOH, chloroform (analytical grade) from Sigma Aldrich, India were purchased and used without further purification.

2.2 Catalyst Preparation

Ruthenium (III) chloride as precursor salt and Poly (N-vinyl-2-pyrrolidone) (PVP as a capping agent) were dissolved in ethylene glycol, which played a dual role for synthesis, as solvent and also as reducing agent was irradiated in microwave reactor (300 W, 200 °C) and cooled down by ice chilled water. Ru/γ-Al_2O_3 nanocatalyst was synthesized by transferring the Ru nanoparticles onto the support**,** redispersed in methanol, mechanically stirred (6500 rpm using Ultraturax) for 24 h, washed with acetone and water to remove the organic and inorganic impurities and dried at 100 °C for 6 h. Dark brown coloured powdered catalyst was calcinated at 300 °C for 8 h in an oven [17].

2.3 Catalyst Characterization

XRD analysis was performed on Bruker D8 (AXE) Powder X-ray diffractometer with Cu-Kα radiation (λ=1.54056 Å) in the range of 5-90 °. TEM images were obtained with a Philips Tecnai – 20, Holland. SEM/EDAX analysis was performed on Shimadzu SSX-550. N_2 adsorption – desorption and hydrogen chemisorptions were carried out by a Micromeritrics ASAP 2010 and Micromeritrics Chemisorb 2750,

USA. SAXS measurements were performed on a Bruker Nanostar instrument equipped with 18 kW rotating anode generator.

2.4 Catalytic Hydrogenation of DB18C6

The hydrogenation of DB18C6 to DCH18C6 was carried out in a 100 ml stainless steel autoclave reactor (Amar Technology, Mumbai. India) built with a thermocouple, hydrogen inlet valve, pressure gauge and magnetic stirrer. 30 ml butanol, 3 g of DB18C6 and known quantity (0.3 g) of prepared activated (1hr in continuous flow of H_2) catalyst (3-5 wt% (as 1 and 2 wt% not found effective) were charged into the reactor at optimum condition (9 MPa H_2, 393 K temperature and 3.5 h).

3. Result and Discussion

3.1. Catalyst Characterization

3.1.1. TEM Analysis

The surface morphology of the Ru/γ-Al_2O_3 (3-5 wt.% Ru) catalyst were studied by TEM. Figure 1 showed that ruthenium nanoparticles imaged as black dark dots and were uniformly dispersed on the γ-Al_2O_3 support, with size of the ruthenium nanoparticles ranging from 1-11 nm. Figure 1(b) and 1(c) indicated the formation of small clusters due to aggregation of nanoparticles at higher (4.5 wt%) metal content.

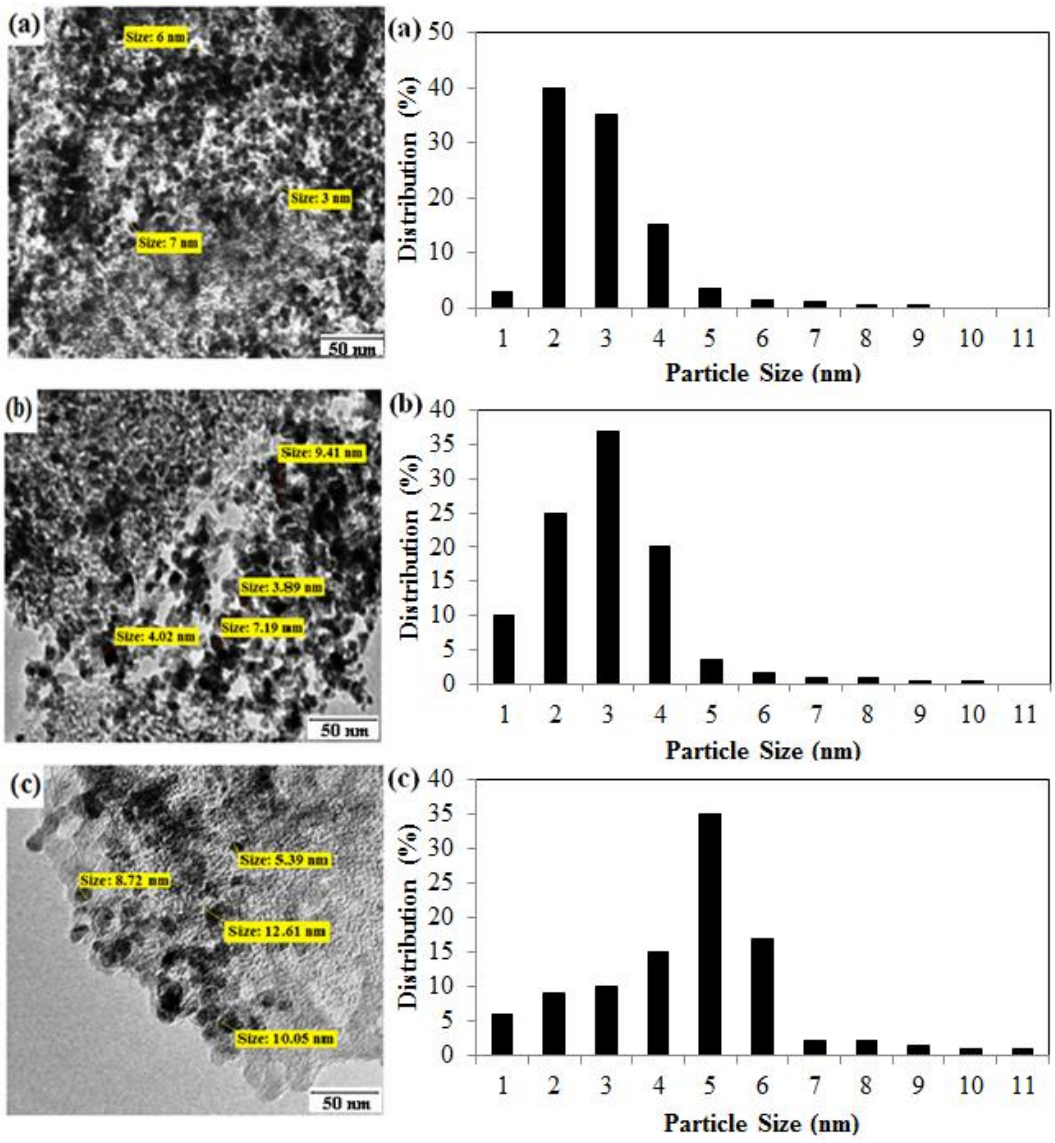

Figure 1. TEM images and particle size distribution of Ru/γ-Al_2O_3 catalysts: a) 3 wt%, b) 4 wt%, and c) 5 wt%.

3.1.2. XRD Analysis

Figure 2 showed the characteristic peaks for ruthenium metal particles around 2θ = 44.08° (101) (highlighted by Δ) of the crystal structure of metal ruthenium (JCPDS file no. 06-0663). The presence of support material γ-alumina was confirmed by the peak at 2θ = 66.5° (JCPDS file No. 10-0425). The average particle size of the ruthenium nanoparticles was calculated from the Scherrer equation, was in the range of 4-14 nm which was closed to the value found from TEM analysis.

3.1.3. SEM and EDAX Analysis

SEM analysis (Figure 3) of 4 wt% Ru/γ-Al_2O_3 revealed that ruthenium nanoparticles of various sizes were uniformly dispersed on the surface, covering the whole surface of γ-Al_2O_3 and the EDAX analysis (Figure 3) of the catalyst indicated the presence of the ruthenium, alumina, oxygen on the surface of the catalyst.

3.1.4. BET Analysis and Metal Surface Area

Table 1 showed that the specific surface area (S_{BET}) of catalyst decreased with increasing ruthenium loading from 3-5 wt%. BET data showed that the metal atoms were mainly deposited on the surface of the γ-alumina, not in the pore of the support. So small change in pore volume (0.24 - 0.156 cm^3/g) was observed and almost all the atom would be accessible to the reaction. To determine ruthenium dispersion and metal surface area (S_M) of the Ru/γ-Al_2O_3

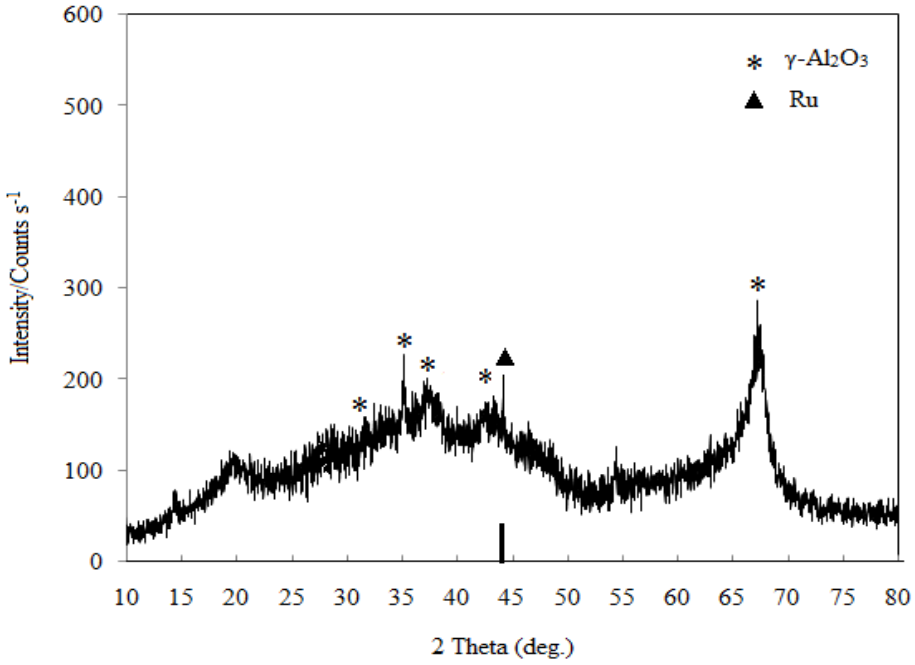

Figure 2. XRD pattern of 4 wt% Ru/γ-Al_2O_3 catalyst.

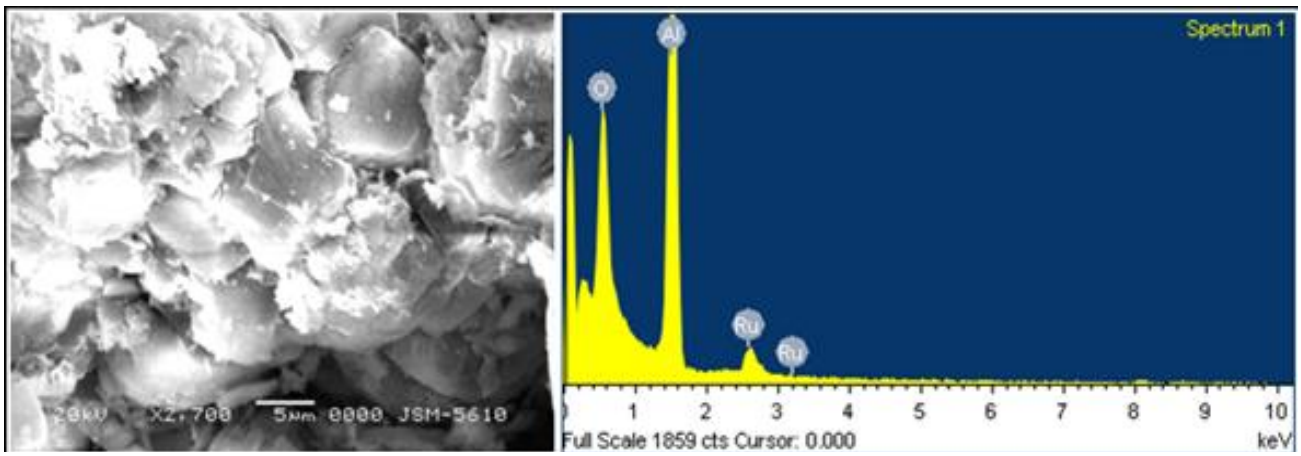

Figure 3. SEM image and EDX analysis of 4 wt% Ru/γ-Al_2O_3 catalyst.

catalyst, hydrogen chemisorptions was carried out (Table 2). The 4 wt.% ruthenium loading indicated maximum active metal surface area on the support then decreased abruptly due to agglomeration of metal atom at higher concentration, which decreased H_2 uptake.

3.1.5. Small-angle X-ray Scattering (SAXS)

Size of the ruthenium nanoparticles dispersed on γ-Al_2O_3 support and commercial catalyst was compared using SAXS (Figure 4). With an increase in concentration of ruthenium from 3-5 wt% metal nanoparticles size was found to increase slightly from 2 nm to 3.5 nm as at the time dispersion tiny particles agglomerated to form larger particles due to lower stabilizer concentration compared to precursor concentration.

4. Catalytic Activity Towards DB18C6 Hydrogenation Reaction

Figure 5 showed the concentration profile of DB18C6 for gas–liquid hydrogenation of DB18C6 to DCH18C6 in presence of continuous flow of H_2 at different time interval. Initially, the reaction pressure, temperature and time were optimized to achieve maximum conversion and was found to be 9 MPa H_2, 393 K temperature and 3.5 h. Table 3 showed the effect of ruthenium loading (3-5 wt%) on DB18C6 conversion. Product mixture was analysed by GC-MS (MS peaks at 372, 201, 171, 143, 99, 72 and 54 a.m.u), NMR [^{1}H: (200 MHz; $CDCl_3$): 1.3-2.0 (m, 16H, —CH_2—), 3.4-3.7(m, 4H, —CH—) and 3.7-3.9 (m, 16H, —CH_2O—)] and liquid XRD (Figure 6). Product analysis showed maximum 96.7% conversion with 100% selectivity towards CSC DCH18C6 using 4 wt% catalyst which indicated better result in terms of selectivity than other reported data. Actually reduced ruthenium has higher density of electron around the atom, and thus larger repulsion to the cyclohexyl ring, the first reduced benzene ring of DB18C6. As the half-hydrogenated crown ether molecule getting close to the Ru catalyst, cyclohexyl ring will be easily pushed to the opposite side and as far as possible to the catalyst surface and produced mainly CSC DCH18C6 (Figure 7).

Table 1. Surface properties of the Ru/γ-Al_2O_3 catalyst.

Entry	BET (m^2/g)	Pore volume (cm^3/g)	Average pore diameter (nm)
Pure γ-Al_2O_3	238	0.24	3.82
3 wt.%	215.57	0.184	3.57
4 wt.%	187.66	0.166	3.71
5 wt.%	165.52	0.156	3.66

Table 2. Hydrogen chemisorptions of Ru/γ-Al_2O_3 catalyst

Entry	Ru wt.%	V (adsorbed gas in ml/g)	Supported metal surface area per g of catalyst (SM, m^2/g cat)
1	3	25.38	42.23
2	4	29.34	47.47
3	5	8.16	11.28

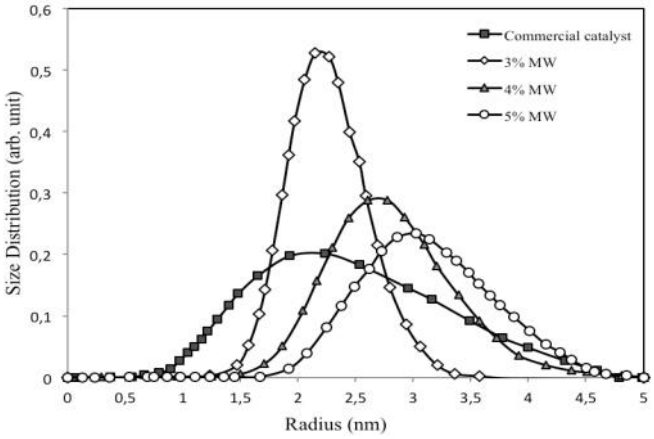

Figure 4. SAXS analysis of supported 4 wt% Ru/γ-Al_2O_3 catalyst and commercial catalyst

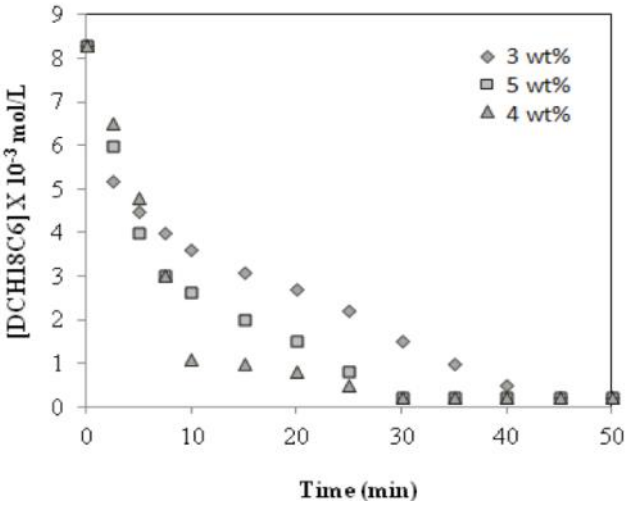

Figure 5. Concentration profile of DB18C6 vs. time for hydrogenation of DB18C6 to DCH18C6. Reaction conditions: temperature 100 ^{0}C; pressure 9 MPa; catalyst amount 0.3 g (3-5 wt% Ru); speed of agitation 160 rpm; 3 g DB18C6 and 30 ml n-Butanol (solvent)

This reaction could be considered as pseudo first order with respect to DB18C6 as concentration of hydrogen will be more compared to DB18C6 (Equation (1)):

$$[C_A] = [C_{A0}]\, e^{-kt} \quad (1)$$

where, C_A = concentration of the reactant, DB18C6 at time t, C_{A0} = initial concentration of the reactant and k = rate constant for the first-order reaction.

Rate constant for first-order reaction can be calculated by Equation (2):

$$\ln [C_A/C_{A0}] = -kt \quad (2)$$

Table 3. Effect of ruthenium loading on the conversion of DB18C6

Entry	Catalysts	(%) Conversion	Initial rate constant k (min^{-1})
1	*5% Ru/γ-Al_2O_3	94.0	0.725
2	3% Ru/γ-Al_2O_3	94.5	0.574
3	4% Ru/γ-Al_2O_3	96.7	0.977
4	5% Ru/γ-Al_2O_3	95.3	0.722

* Ru/γ-Al_2O_3 commercial catalyst

It was found from Figure 5 that 80-90% reduction occurs within 10 min of reaction time. From the ln (C_A/C_{A0}) versus t plot (not shown), the initial rate constant (up to 10 min of reaction time) was calculated at different ruthenium loading on the catalyst. It was found from Table 3 that the rate constant increased linearly with increasing ruthenium loading from 3 to 4 wt% (0.574 to 0.997 min^{-1}) and then decreased at 5 wt% metal loading (0.722 min^{-1}).

Comparing the catalytic activities with different loading ruthenium, 4 wt% ruthenium loading was considered to be the optimum because it provided the highest % conversion of

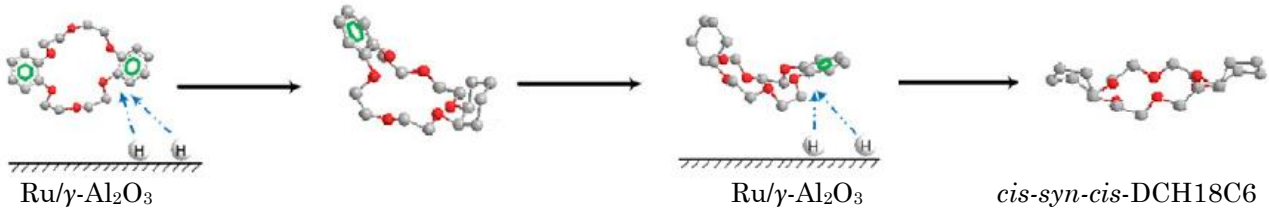

Figure 7. Mechanism of formation of CSC DB18C6 on Ru/γ-Al_2O_3 catalyst

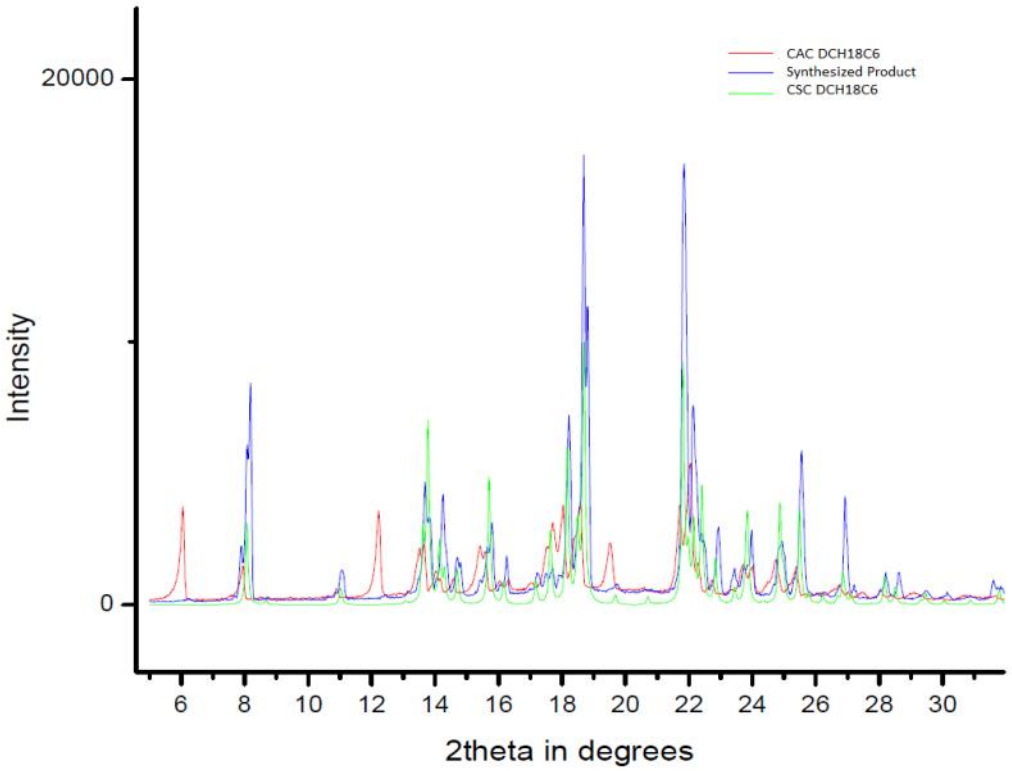

Figure 6. Liquid XRD analysis of CAC & CSC DCH18C6 and synthesized product

DB18C6 (even better than 5 wt% commercial catalyst). The smaller ruthenium nanoparticles (up to 4 wt% loading) would be in bulk of the active surface area and with an increase of metal loading, a decrease in the number of small particles is seen in the structure region, which was responsible for lower catalytic activity. Larger loading also led to more agglomeration and larger average particle size. TEM images (Figure 1b) showed that the 4 wt% ruthenium loading, though forming metallic nanoclusters to some extent, was the optimum because the ruthenium particles were not too dense and dispersed uniformly on the support. It was hypothesized that this provided the maximum active sites for hydrogenation of DB18C6. Chemisorptions results (Table 2) also showed that 4 wt% ruthenium loaded catalyst had the highest (S_M = 47.47 m^2/g_{cat}) active metal site to carry out the hydrogenation reaction at faster rate. It is also found from Figure 5 that the 5 wt% Ru/γ-Al_2O_3 showed higher activity than that of 3 wt% Ru/γ-Al_2O_3 although the metal surface area of 3 wt% ruthenium loaded catalyst (42.23 m^2/g) is higher than that of 5 wt% ruthenium loaded catalyst (11.28 m^2/g). It indicated that ruthenium nanoclusters formed at higher (5 wt%) metal loading (Figure 1c) were highly active sites for hydrogenation reaction, which resulted higher conversion (95.3%) and larger initial rate constant (0.722 min^{-1}).

5. Conclusion

Supported ruthenium metal nanocatalyst was synthesized by microwave irradiated solvothermal technique. Synthesized catalysts activity was then successfully tested for the hydrogenation reaction of DB18C6 to DCH18C6. 4wt% Ru/γ-Al_2O_3 showed 96.7% conversion with 100% selectivity towards CSC DCH18C6 which exhibited even better result compared to 5wt% commercial catalyst.

References

[1] Blasius, B., Klein, W., Schon, U.J. (1985). *Radioanal. Nucl. Chem.,* 89: 389-398.

[2] Kumar, A., Mohapatra, P.K., Pathak, P.N., Manchanda, V.K. (1997). *Talanta*, 45: 387-395.

[3] Yost, T.L. Jr, Fagan, B.C., Allain, L.R., Barnes, C.E., Dai, S., Sepaniak, M.J., Xue, Z. (2000). *Anal. Chem*., 72:5516-5519.

[4] Landré, P.D., Lemaire, M., Richard, D., Gallezot, P. (1993). *J. Mol. Catal*., 78:257-261.

[5] Lemaire, M., Guy, A., Chomel, R., Foos, J. (1991). *J. Chem. Soc. Chem. Commun*., 1552-1154.

[6] Guyon, V., Landre, P.D., Guy, A., Foos, J., Lemaire, M. (1992). *Chem. Lett*., 723-726.

[7] Pedersen, C. J. (1972). *Org. Synth*., 52: 66-74 .

[8] Yakshin, V.V., Fedorova, A.T., Laskorin, B.M. (1986). *Russ. Chem. Bull*., 35: 463-467

[9] Gurskii, R.N., Istratova, R.V., Kirova, A.V., Kotlyar, S.A., Ivanov, O.V., Lukyanenko, N.G. (1988). *J. Org. Chem. USSR* (Engl. Transl.)., 24: 543.

[10] Landré, P.D., Richard, D., Draye, M., Gallezot, P., Lemaire, M. (1994). *J. Catal*., 147: 214-222.

[11] Gao, J., Chen, S., Chen, J. (2012). *Catal. Commun*., 28:27-31.

[12] Zawadzki, M., Okal, J. (2011). Mater. Res. Bull., 43: 3111-3121.

[13] Okal, J. (2010). *Catal. Commun*., 11: 508-512.

[14] Antonetti, C., Oubenali, M., Galletti, A.M.R., Serp, P.,Vannucci, G. (2012). *Appl. Catal. A: Gen.*, 99: 421-422.

[15] Rini, A.S., Ramdiman, S., Yarmo, M.A. (2012). *Adv. Mater. Research*, 364: 283-287.

[16] Suryawanshi, Y.R., Chakraborty, M., Jauhari, S., Mukhopadhyay, S., Shenoy, K.T., Shridharkrishna, R. (2013). *Cryst. Res. Technol*., 48: 69-74.

[17] Nandanwar, S.U., Chakraborty, M., Mukhopadhyay, S., Shenoy, K.T. (2011). *Cryst. Res. Technol.*, 46: 393-399.